

# NUMERICAL SIMULATION OF WATERSPOUTS OBSERVED IN THE TYRRHENIAN SEA

## 4M.1

by G. J. Tripoli (1)\* , Carlo Medaglia (2), A. Mugnai (2) , Eric Smith (3)

(1) University of Wisconsin, USA (2) Istituto di Scienza dell'Atmosfera e del Clima, CNR, Via Fosso del Cavaliere 100, 00133 Roma, Italy (3) NASA Goddard, USA

## 1. INTRODUCTION

This study was motivated when the authors were traveling on a ferry from Livorno, Italy to Bastia, France on the island of Corsica on route to the 4<sup>th</sup> Plinius conference to be held in Ajaccio. The early morning excursion, departing Bastia under cool, calm, clear sky conditions encountered a line of congestus over the water that were spawning a spectacular display of numerous waterspouts (see figure 1) about midway over the Tyreanean Sea, just south of the island of Capraia. The simple lack of interest in the spouts by the regular ferry travelers suggested, that this event was probably common place. The early morning timing of the spouts and the linear geometry of the congestus cloud system suggested to the authors that a land breeze was the likely mechanism for generating a shear line capable of causing this event.



Figure 1: Waterspout observed at 9:28 UTC, 30 September, 2003 facing east from a position southeast of the island of Capraia. Notice that this water spout has a condensation funnel reaching over half of the way down from the 600-800m cloud base, or about 300-500m.

Because of the predictability of a simple land breeze was likely high, the authors felt that it might be possible to model this event explicitly, by simulating the formation of the land breeze using a model initialized from an ECMWF analysis and with locally sufficient resolution, through two-way grid nesting, to represent the synoptic progression on the macro scale, the land breeze on the mesoscale, the congestus on the cloud scale, and the waterspouts on the micro scale. This was accomplished using the University of Wisconsin Nonhydrostatic Modeling System (Tripoli, 1992). Figure 2 depicts the 8 two-way nested grid system used.

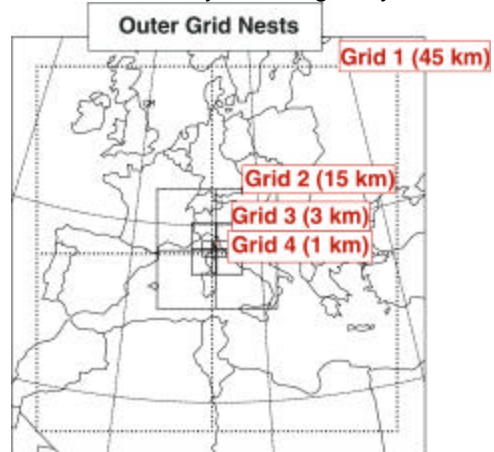


Figure 2: Grid nesting system used depicting the first four nests. Spacing for grid 1-grid 8 is: (1) 45 km, (2) 15 km, (3) 5 km, (4) 1 km, (5) 200m, (6) 40m, (7) 8m, (8) 2m

## 2. EXPERIMENT DESIGN

The model employed for this study was the UW-NMS (Tripoli, 1992, 2006). This is a time-split quasi-compressible nonhydrostatic model featuring a spherical grid and variably stepped topography. The model was initialized from the ECMWF analysis of 12 UTC 29 September,

\* Corresponding author address: Gregory Tripoli, Univ. of Wisconsin- Madison, Dept of Atmospheric and Oceanic Sciences, Madison, WI 53706, Tripoli@aos.wisc.edu

2003, or about 22 hours prior to the waterspout observations.

The equations of motion were originally formulated in the enstrophy conserving form:

$$\frac{\partial u_i}{\partial t} = -\mathbf{e}_{i,j,k} u_j (z_k + f_k) - \frac{\partial k}{\partial x_i} - \mathbf{q} \frac{\partial \mathbf{p}}{\partial x_i} + \mathbf{d}_{i3} g \frac{\mathbf{q}}{\mathbf{q}_o} + F_1(u_j, \mathbf{q}) + F_2(u_i)$$

where  $\mathbf{u}_i$  is the velocity tensor,  $f_j$  is the Coriolis tensor,  $\mathbf{q}$  is the potential temperature,  $g$  is the acceleration of gravity,  $\mathbf{d}_{ij}$  is the Kronecker delta function, and  $\mathbf{p}$  is the Exner function

$$\left( \mathbf{p} = c_p \left( \frac{p}{1000mb} \right)^{\frac{R}{c_p}} \right), \text{ where } p \text{ is pressure. The}$$

vorticity vector is defined as:

$$\mathbf{z}_i = \mathbf{e}_{i,j,k} \frac{\partial u_j}{\partial x_k},$$

the kinetic energy as:

$$k = \frac{1}{2} (u_i^2),$$

and the permutation tensor ( $\mathbf{e}_{i,j,k}$ ) is defined as:

$$\mathbf{e}_{i,j,k} = \begin{cases} 0 & \text{if } i=j, \text{ or } j=k, \text{ or } i=k \\ 1 & \text{if } i,j,k \text{ are } 1,2,3 \text{ or } 2,3,1 \text{ or } 3,1,2. \\ -1 & \text{if } i,j,k \text{ are } 3,2,1 \text{ or } 2,1,3 \text{ or } 1,3,2 \end{cases}$$

The quantities  $F_1$  and  $F_2$  are eddy viscosity based physical turbulence and a numerical smoother respectively. Perturbations are relative to an arbitrary dry hydrostatic base state obeying the ideal gas law that is designated by the subscript "o".

This formulation has the advantage of providing for a unique numerical definition of the three components of vorticity that is consistently used by each of the three equations of motion. That numerically couples the three equations of motion in the form of a true vector acceleration. Moreover, employing differencing techniques of Arakawa and Lamb (1981), this form enables strict conservation of vorticity and the removal of numerical sources of enstrophy in all three dimensions. In this sense, this is an optimal differencing method for the representation of a vortex, especially in cases where the model resolution may be marginal. In the case of nonlinear flow, numerical enstrophy cascade is controlled in three-dimensions, enabling a better simulation of the envelope of solutions occurring within a chaotic flow regime.

The model also contained acceleration terms for centrifugal force affecting rain droplets,

which were modeled using a two moment distribution. Sea spray was parameterized based on a scheme of Andreas(1998)

### 3. RESULTS

Simulations were initially performed with the first 4 grid meshes only, having a maximum resolution of 1km. We tried both ECMWF and NCEP GFS at both 0000UTC and 1200 UTC for 29 September, 2003 to provide initial conditions, but determined the ECMWF at 00 UTC gave the most promising setup for shear line tornadoes. The mesoscale flow system formed a long shear line on the lee side of Corsica as a result of the distortion of barrier flow by the nocturnal downslope flow regime. WISHE forcing by strong winds upwind of Corsica brought positive CAPE values around the island to the Capraia island region where congestus cells were initiated. Figure 3 depicts the CAPE along the shear/convergence line that was built and the initial cloud formation.

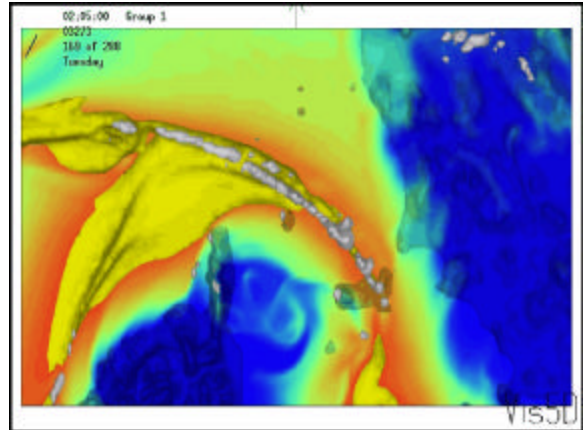


Figure 3: Cape (yellow) and cloud field (white) simulated on grid 4 at 0205 UTC, 29 September, 2003.

We added a 5<sup>th</sup> nest of 200 m resolution over a region along that line and simulated the formation of multiple vortices associated with the developing convection over the line. We then added the 6<sup>th</sup> grid of 40 m resolution to better resolve the vortices. Figure 4 depicts the family of vortices that we attributed to the formation of waterspouts.

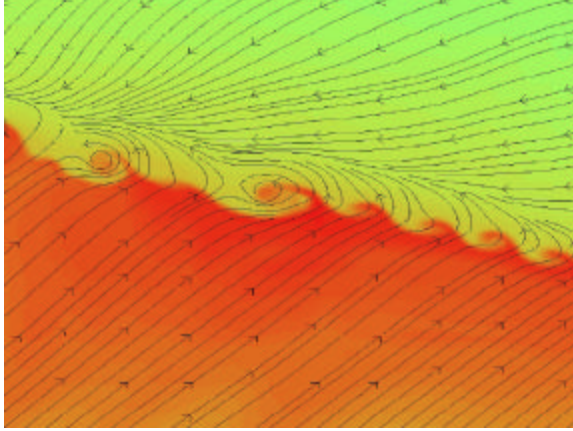


Figure 4: A family of vortices, depicted on grid 6.

Next we added a 7<sup>th</sup> grid of 8 m resolution during the lifecycle of one of the more interesting vortices scripted to move with the vortex. This produced a good deep vortex, but tangential velocities were too weak to create a condensation funnel.

We added an 8<sup>th</sup> grid of 2m resolution over a lateral domain of 500 m around the vortex to better resolve the waterspout vortex. This did allow the vortex to be only slightly more intense and a very small 1 grid point, i.e. 100 m deep funnel formed. Tangential winds approached 15 m/s in the funnel. Figure 5 depicts this simulated funnel.

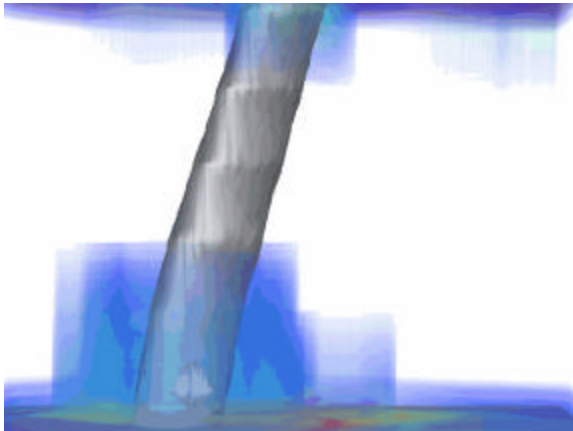


Figure 5: Grid 8 vorticity field and cloud (blue shading).

#### 4. VORTICITY CONFINEMENT

We employed a vorticity confinement scheme developed by Steinhoff and Underhill (1994). The original equations of motion were modified as:

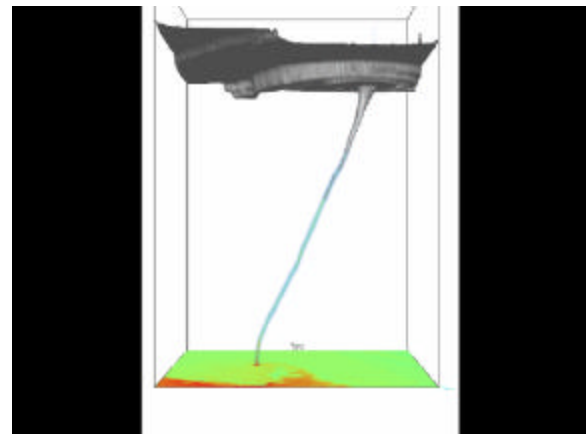
$$\frac{\partial u_i}{\partial t} = -\mathbf{e}_{i,j,k} (u_j + \mathbf{w}_j) (\mathbf{z}_k + f_k) - \frac{\partial k}{\partial x_i} - \mathbf{q} \frac{\partial \mathbf{p}}{\partial x_i} + \mathbf{d}_{i3} g \frac{\mathbf{q}}{\mathbf{q}_0} + F_1(u_j, \mathbf{q}) + F_2(u_i)$$

where,

$$\mathbf{w}_j = \mathbf{e} \frac{\bar{\nabla} \mathbf{p}}{|\bar{\nabla} \mathbf{p}|}$$

is the vorticity confinement term. The parameter  $\mathbf{e}$  was set to 1 for these experiments. Little sensitivity was found to varying  $\mathbf{e}$  as Steinhoff predicted. The theory behind this modification is that downscale turbulent cascade of vorticity is blocked by inertial stability, but numerical schemes, even the enstrophy conserving scheme that we employ, cannot resolve these effects. When scales are truncated, one inevitably loses vortex energy out the bottom preventing the rollup of a tight vortex in a turbulent atmosphere. This artificial vorticity source is meant to counter the natural loss of vorticity confinement. Steinhoff tested this term against laboratory measurements in a wind tunnel and found extremely good results. Note that no “net” vorticity is added to the system overall. In fact, the term was shown by Steinhoff to be self-adjusting so as not to cause spinup of a vortex unnaturally.

Our tests seemed to confirm Steinhoff's predictions of sensitivity to  $\mathbf{e}$  and the implications of confinement. Once we put this term in, our vortex strengthened to over 20 m/s tangential wind and the pressure within the vortex dropped by 35 hPa, allowing the condensation funnel to descend 350m. Figure 6 depicts this result.



Grid 8 with vorticity confinement, cloud as white surface and blue is vorticity surface.

#### 5. FUNNEL DYNAMICS

Some interesting features of the condensation funnel dynamics were found in these experiments. First, it was found that within the condensation funnel, the constant  $q_e$  environment of the updraft made the vertical stability moist neutral. This drew cloudy air, including developing rain drops, from the cloud above downward into the low pressure within the condensation funnel. The funnel below the condensation funnel had generally positive or upward spiraling helicity. Hence in the region of the condensation funnel, the outer funnel was moving up and the inner funnel was moving down. In addition, the rotation vector of the vortex seldom pointed directly up. Hence one half of the vortex was rotating up and the other down. Only the helicity could distinguish the true direction of the spiral.

Experiments were also performed with the effects of centrifugal force on the rain droplets. This had a strong sorting effect, moving the larger droplets to the outside, lessening the water loading effects on the funnel interior. These results will be explained further at the oral presentation and in a forthcoming journal paper.

#### 1. Conclusions

The results demonstrated the high potential for waterspout formation in response to mesoscale flow regimes set up by channeled flow in the Mediterranean region. Model predictions of the spouts were not precise in time and location, but they did show the likelihood of shear-line tornadoes in the region quite well. Perhaps in the form of an ensemble of mesoscale simulations, a high resolution model could better define the overall potential for such development.

This study also led to some new understanding of funnel dynamics. In particular, the role of vorticity confinement in producing funnels in a turbulent environment was implied. We are currently studying vorticity confinement and the realm over which it can be included. As of this writing, our results suggest that the term has little effect on large scale flow systems when added and does not affect the waterspout lifecycle as it dissipated after 11 minutes, just as it had without the term.

Finally, our spout simulations have provided new, interesting insight into the dynamics within a tornadic vortex. In particular the vertical circulation in response to a condensation funnel is interesting, as well as the droplet sorting effects on buoyancy.

---

## 6. REFERENCES

- Andreas, E. L., 1998: A new sea spray generation function for wind speeds up to 32 ms-1. *J. Phys. Oceanography*, 28, 2175-2184
- Steinhoff, J. and D. Underhill, 1994: Modification of the Euler equations for "vorticity confinement": Application to the computation of interacting vortex rings. *Phys. Fluids*, 6, 2738-2744
- Tripoli G. J., 1992: A Nonhydrostatic Mesoscale Model Designed to Simulate Scale Interaction, *Mon. Wea. Rev.*, **120**, 1342-1359.

## ACKNOWLEDGMENTS

The authors would like to thank Dr. John Steinhoff for his input to this study. This work is supported by a grant through NASA Earth Sciences Division's Precipitation Measuring Mission (PMM) research program.

